Journal Name

RSCPublishing

View Article Online
DOI: 10.1039/C4SC01603C

ARTICLE

Glucose oxidase triggers gelation of *N*-hydroxyimide-heparin conjugates to form enzyme-responsive hydrogels for cell-specific drug delivery†

Cite this: DOI: 10.1039/x0xx00000x

Received 00th January 2012,
Accepted 00th January 2012

DOI: 10.1039/x0xx00000x

www.rsc.org/

Teng Su,[a] Zhou Tang,[a] Hongjian He,[a] Wenjun Li,[a] Xia Wang,[a] Chuanan Liao,[a] Yao Sun[b] and Qigang Wang*[a]

A new strategy for creating enzyme-responsive hydrogels by employing an *N*-hydroxyimide-heparin conjugate designed to act as both an enzyme-mediated radical initiator and an enzyme-sensitive therapeutic carrier is described. A novel enzyme-mediated redox initiation system involving glucose oxidase (GOx), *N*-hydroxyimide-heparin conjugate and glucose is reported. The GOx-mediated radical polymerization reaction allows the mild and quick formation of hydrogels with excellent flexibility in modulating physical and chemical characteristics. The heparin-specific enzymatic cleavage reaction enables the delivery of cargo from the hydrogel in amounts that are controlled by the environmental levels of heparanase, which is frequently associated with tumor angiogenesis and metastasis. The formed hydrogels can realize cell-specific drug delivery by targeting cancer cells that are characterized by heparanase overexpression, while showing little toxicity toward normal cells.

Introduction

Drawing endless inspiration from Mother Nature, scientists have been persistently dedicated to designing and developing new smart systems capable of responding to environmental stimuli in a controllable and predictable fashion, while mimicking the feedback-controlled processes that are inherent to biological systems.[1-8] In the past few years, a variety of elegantly devised stimuli-sensitive hydrogels that are responsive to light,[9,10] γ-radiation,[11] temperature,[12] pH,[13] redox,[14] enzymes,[15,16] and other chemical or physical external stimuli,[17,18] have been introduced. Because enzymes are vital components in many biological pathways, enzyme-responsive hydrogels have been attracting growing interest for their intriguing physiochemical properties and their potential uses in diagnostics and therapeutics. The enzyme-triggered sol-gel transition has been actively investigated for the formation of non-covalent molecular hydrogels[19-23] and enzymatically cross-linked hydrogels[24-27] with exciting biological functionalities. Recently, enzyme-mediated radical polymerization has also emerged as another promising, benign method of providing high efficiency and selectivity when fabricating bioactive hydrogels.[28-30] For example, an eminent enzyme-mediated radical initiation system involving the specific reaction between glucose oxidase (GOx) and β-D-glucose in the presence of Fe^{2+} enables the formation of hydroxyl radicals that are capable of efficiently initiating chain polymerization to generate cytocompatible hydrogel scaffolds or sequential multilayers.[29,31-33]

Inspired by these pioneering studies, we unexpectedly noticed that an *N*-hydroxyimide compound, *N*-hydroxy-5-norbornene-2,3-dicarboximide (HONB), can be readily reduced with β-D-glucose in the presence of GOx, which rapidly forms a carbon-centered radical. Excitingly, this species can initiate the polymerization of acrylamide in an aqueous environment at room temperature (approx. 25 °C). To the best of our knowledge, this mild ternary enzymatic initiation system has not been reported. These results stimulated us to explore the feasibility of using GOx-mediated radical polymerization to fabricate biologically derived, enzyme-responsive hydrogels. A main component of our hydrogel, heparin, is a highly sulphated polysaccharide belonging to the family of glycosaminoglycans (GAGs).[34,35] Because heparin has a unique composition with repeating disaccharide units of hexuronic acid and glucosamine, it shows specific binding to many growth factors and cytokines, as well as susceptibility toward heparanase, which is frequently associated with tumor angiogenesis and metastasis.[36-38] Many heparin-based systems with different architectures have been developed and have functioned as new biomaterials for drug delivery and extracellular matrix mimicking.[39-43] The conjugation of anticancer drugs to heparin shows comparable even somewhat improved drug efficacy relative to free drugs.[41] Heparin that is functionalized with HONB can serve as a substrate for enzyme-mediated polymerization. Therefore, hydrogels based on the unimolecular combination of an enzymatic polymerization initiator (EPI) and an enzyme-sensitive carrier might enable the development of smart cargo-delivery systems.

Herein, we report a new strategy for creating an enzyme-responsive heparin-containing hydrogel as a cell-specific drug delivery system that utilizes two orthogonal enzyme reactions. The GOx-mediated polymerization reaction allows the mild and

View Article Online
DOI: 10.1039/C4SC01603C

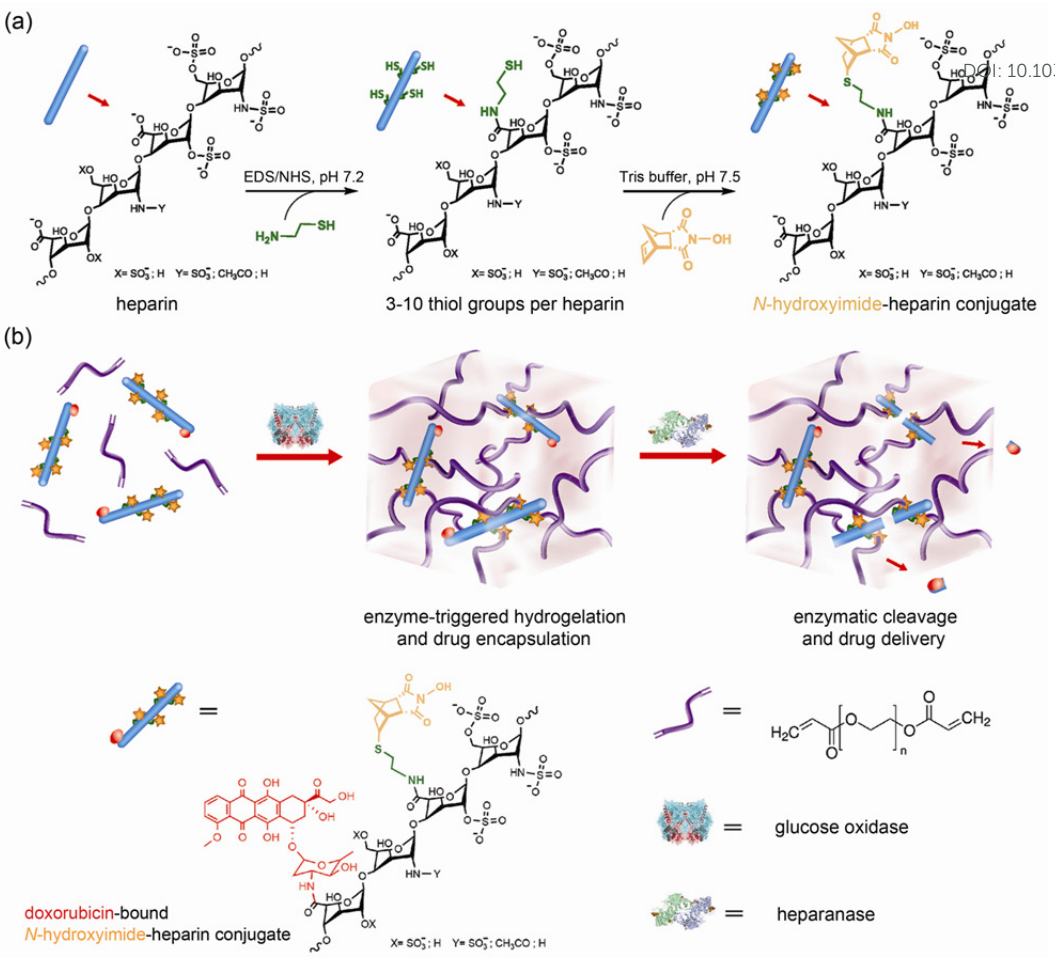

Fig. 1 (a) Synthesis of the *N*-hydroxyimide-heparin conjugate. (b) Enzyme-responsive hydrogel is formed by GOx-mediated radical polymerization using the DOX-bound, *N*-hydroxyimide-heparin conjugate as both an EPI and an enzyme-sensitive cargo carrier. The gel network can be specifically degraded by heparanase which is a key protein overexpressed in tumor region, resulting in the targeted delivery of anticancer drugs (red balls).

quick formation of hydrogels at room temperature with independent tunability of the gelation time and the physical properties. The heparin-specific enzymatic cleavage reaction enables the delivery of drugs from the hydrogel in amounts that are controlled by the environmental levels of heparanase. Rational engineering can produce biological molecules that contain both the *N*-hydroxyimide moieties for enzyme-mediated radical initiation and the covalently bound drug molecules (Fig.1); thus, the enzyme-mediated radical polymerization and cleavage reactions can be used to create elaborate hydrogel-based therapeutic carriers that target the abnormal cells (*e.g.*, malignant cancer cells) that overexpress specific enzymes. Toxic side-effects and premature release are major problems that plague the clinical use of many therapeutic drugs. Addressing this challenge, our hydrogel system discriminates enemy from friend. Our system can release drugs that are responsive to the target enzyme that is overexpressed by cancer cells, while becoming inert when encountering normal cells due to stable amide anchoring of anticancer drug molecules in the gel network. This anchoring minimizes the adverse effects caused by the undesired release of drugs onto normal cells.

Results and discussion

The multifunctional enzyme-responsive carrier is synthesized via a two-step functionalization of the heparin backbone with up to ten *N*-hydroxyimide groups (Fig. 1a). Cysteamine is employed to react stoichiometrically with the heparin carboxylic groups to introduce thiol groups. By precisely controlling the molar ratios between the reactants, we are able to obtain heparin-cysteamine conjugates with defined amounts of thiol groups and with high yields of over 90% (see Experimental section, Fig. S1 and S2 in ESI†). Then, the thiol-containing heparin-cysteamine conjugates, after being activated in the presence of 1, 4-dithio-D-threitol (DTT), are reacted with excessive HONB to ensure complete substitution via a thiol-norbornene Michael-type addition. The purified *N*-hydroxyimide-heparin conjugate (HepSN) is obtained after exhaustive dialysis and lyophilization to afford an off-white solid with an overall yield of 76 %. Characterizations using proton nuclear magnetic resonance (^{1}H NMR) and Fourier transform infrared spectroscopy (FTIR) confirm the incorporation of the *N*-hydroxyimide moiety into the heparin backbone (Fig. S3 and S4, ESI†). In the ^{1}H NMR, the signals that characterize heparin are observed: the resonances of

View Article Online
DOI: 10.1039/C4SC01603C

protons at 5.34, 3.98, and 3.69 ppm are assigned to H1, H5, and H4, respectively, in the GlcNS6S unit of heparin; the signal at 4.18 ppm correlates with H3 in the IdoA2S unit; and the characteristic proton peak of the methyl group in the GlcNAc unit appears at 2.01 ppm. Moreover, the simultaneous appearance of the α-proton peak of the thioether at 2.40 – 2.51 ppm and the weak N-OH proton peak at 10.25 ppm is observed along with the disappearance of the alkene proton peaks of norbornene at 6.05 ppm; these features indicate the complete conversion of the norbornenes and thiols to thioethers and the successful incorporation of *N*-hydroxyimide moieties.[44,45] The FTIR analysis of the *N*-hydroxyimide-heparin conjugate also reveals amide I carbonyl stretching at 1640 cm^{-1}, C-S stretching at 951 cm^{-1}, and a weak N-OH bending vibration at 1544 cm^{-1} that overlap with the amide II N-H bending and C-N stretching,[46] which is consistent with the ^1H NMR characterization. For drug loading, the obtained *N*-hydroxyimide-functionalized heparin can be further conjugated with doxorubicin (DOX), one of the most widely used anticancer drugs, via amide bonding with the remaining carboxylate groups (Fig. 1b). Notably, the functionalization of heparin with between three and ten *N*-hydroxyimide groups is suitable to trigger hydrogelation because more modification will considerably decrease the solubility of the *N*-hydroxyimide-heparin conjugate in water after drug loading, thus hampering its further use as an EPI in the subsequent enzyme-mediated radical polymerization.

To form a hydrogel, the *N*-hydroxyimide-heparin conjugate (5 wt %) and poly (ethylene glycol) diacrylate (PEGDA, 5 wt %) are simply dissolved in deionized water and mixed together with glucose (50 mM) in a sealed vial. Upon the final addition of GOx (4 μM) to the as-prepared homogeneous solution, gelation occurs within 30 min at room temperature to yield a self-supporting hydrogel (designated hereafter as HepSN gel). The hydrogel formation is confirmed by detailed analysis. Rheological measurement in time-sweep mode reveals the gelation kinetics of such a system by monitoring the storage modulus (G') and loss modulus (G'') as a function of time (Fig. S5, ESI†). A crossover point between G' and G'' appears at 7.5 min, which can be defined as the gelation time ($T_{gelation}$) for this system.[47] Electron paramagnetic resonance (EPR) spectroscopy analysis provides direct evidence that this gelation proceeds through an enzyme-mediated radical initiation mechanism. The initiating radical, formed in the HepSN-GOx-glucose ternary system aqueous solution, can be observed within 5 min after the adduction with α-(4-pyridyl-1-oxide)-*N*-tert-butylnitrone (POBN). The spectrum of this species shows a triplet of doublets (hyperfine splitting constants: a^H=2.5 G, a^N=15.5 G, and g=2.0053) that are similar to those derived from HONB (Fig. S6 and S7, ESI†). The successful initiation of radical polymerization has also been supported by the active propagating radicals observed in the EPR spectra of the precursor solution with PEGDA or other vinyl monomers (Fig. S8, ESI†). The final acrylate conversion, as determined using *in situ* NMR analysis, reaches approximately 98% after 30 min of reaction (Fig. S9, ESI†). According to the literature,[48-50] the GOx-mediated radical initiation process can be divided into two half-reactions: a reductive step and an oxidative step. In the reductive half reaction, GOx mediates the oxidation of β-D-glucose to D-glucono-δ-lactone by reducing its flavin adenine dinucleotide (FAD) ring to the hydroquinone form ($FADH_2$) that carries two electrons and two protons from β-D-glucose. In the oxidative half reaction, $FADH_2$ can presumably donate its electrons to the *N*-hydroxyimide moieties and revert to the initial quinone form (FAD), yielding radicals that can initiate the polymerization of monomers. The residual dissolved oxygen in the gelation system can also compete for electrons to generate H_2O_2, thereby suppressing the polymerization. This reaction may contribute to an induction period before the gelation point occurs, which is consistent with the time-sweep rheological measurement. We found that the gelation could be realized after degassing procedure, indicating that this GOx-mediated radical polymerization can take place under anaerobic conditions. Therefore, the H_2O_2 generation during hydrogelation could be avoided, which would be beneficial when fabricating functional hydrogels for biological uses. The conjugation of DOX molecules to the *N*-hydroxyimide-heparin conjugate has no significant effect on its ability to trigger gelation (Fig. S10, ESI†). Visualization of the DOX-loaded hydrogel (denoted hereafter as Hep(DOX)SN gel) by confocal laser scanning microscopy (CLSM) indicates that the drug molecules are connected to the heparin-based carriers and are distributed evenly in the gel network (Fig. S11, ESI†).

Precise control of the reaction conditions allows the users to tune the gelation time, crosslinking density and resulting physical properties, as illustrated in Fig.2. We employed a one-way analysis of variance procedure to determine whether each controlling parameter has a significant effect on the values of $T_{gelation}$ and G', respectively.

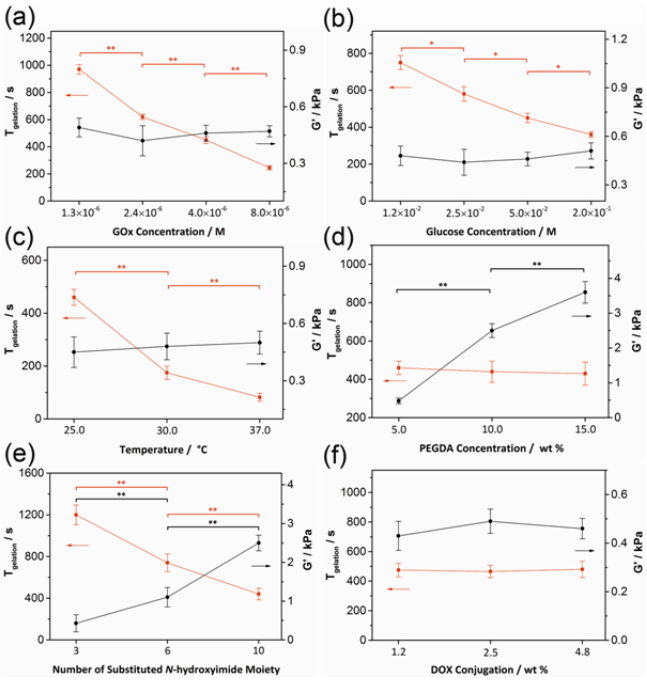

Fig. 2 The gelation time of the hydrogel can be tuned independently of the mechanical properties by adjusting the concentration of one of the following: (a) GOx, (b) glucose, and (c) temperature. (d) The storage modulus can be tuned independently of the gelation time by solely varying the monomer concentration. (e) The number of substituted *N*-hydroxyimide moieties regulates the gelation time and storage modulus simultaneously (PEGDA: 10 wt %). (f) The DOX conjugation can be adjusted without affecting the gel properties. Unless otherwise stated, the hydrogels are prepared from HepSN with ten substituted *N*-hydroxyimide moieties (5 wt %) and PEGDA (5 wt %) in the presence of GOx (4 μM) and glucose (50 mM) at 25 °C. Data represent the mean ± standard deviation (n=3), where * $P < 0.05$ and ** $P < 0.01$.

Increasing the concentration of GOx or glucose at a constant polymer weight percentage leads to faster gel formation with a similar storage modulus. Therefore, the gelation time can be tuned independently of other parameters (Fig. 2a and 2b). Amazingly, the formation of our hydrogel is significantly accelerated by simply elevating the working temperature from 25 to 37 °C (Fig. 2c). Inspired by this result, we have prepared a fully developed hydrogel under physiological conditions within 4 min (determined by vial-tilting method).

The matrix stiffness can be tuned irrespectively of the gelation time just by varying the PEGDA concentration from 5 to 15 wt % (Fig. 2d). Moreover, incorporating the same amount of heparin with different types of conjugation in our hydrogel allows us to exert simultaneous control over both the gelation time and the gel strength (Fig. 2e) and to achieve different amounts of drug encapsulation without affecting the gel properties (Fig. 2f). Increased *N*-hydroxyimide conjugation leads to a higher concentration of initiating radicals and crosslinking degree in the gelation system, thereby reducing the gelation time and increasing the mechanical strength. These results indicate that the introduced gelation strategy endows the as-prepared hydrogel with excellent flexibility in modulating physical and chemical characteristics, which is ideal for biological applications with advanced microstructuring requirements.[51,52]

For cargo release, the DOX-bound heparin chain that is encapsulated into the hydrogel can be cleaved depending on the environmental concentration of heparanase. We first investigated the enzyme-induced drug (the heparin-DOX conjugate) release kinetics from the Hep(DOX)SN hydrogel in the presence of a solution containing heparinase I at pH 6.8 that mimics the tumor microenvironment. The DOX-conjugated non-heparanase-responsive PEG hydrogel (PEG-DOX gel) was used as the reference material (see Experimental section in ESI†). Because the crosslinking degree of the gel network greatly affects the release profile,[40] we investigated the Hep(DOX)SN and PEG-DOX gels, which have similar storage moduli and correspondingly similar crosslinking degrees (Fig. S12, ESI†). In the absence of heparinase I, neither the Hep(DOX)SN gel nor the PEG-DOX gel showed drug release within 60 h. Interestingly, in the presence of 5 U mL^{-1} of heparinase I at 37 °C, approximately 46% of DOX was released within 60 h from the Hep(DOX)SN gel, while no drug release was observed from the reference PEG-DOX gel, suggesting that the drug release is caused by enzyme cleavage (Fig. S13, ESI†). Increasing the enzyme concentration speeds up the release process and increases the final release content (Fig. S14, ESI†).

To evaluate the potential of the Hep(DOX)SN gel for cell-specific drug delivery, we examined its cytotoxicity against three cell lines: HeLa, HepG2, and NIH-3T3 cells. HeLa and HepG2 are well-established cancer cells that express high and low amounts of heparanase, respectively.[37] NIH-3T3 cells are chosen from a mouse embryonic fibroblast cell line that does not express heparanase. The drug-loaded gel particles (approx. 500 μm in diameter) were used to provide sufficient direct contact with the cells during incubation. As shown in Fig. 3a–c, the free DOX is effective at combating HeLa and HepG2 cancer cells; however, it also poses a great threat to NIH-3T3 cells because of its intrinsic non-specificity. Interestingly, the Hep(DOX)SN gel shows dose-dependent cytotoxicity against both HeLa cells (Fig. 3a) and HepG2 cells (Fig. 3b). The drug-free *N*-hydroxyimide-heparin conjugate as well as the HepSN gel are not toxic, as evidenced by the high cell viability that was maintained after 60 h exposure (Fig. 3d and Fig. S15 in ESI†), demonstrating that the cytotoxicity of the Hep(DOX)SN gel is due to DOX. For HepG2 cells with their low heparanase expression, the IC_{50} (i.e., inhibitory concentration to produce 50 % cell death) value of the Hep(DOX)SN gel was determined to be 4.8 μM, which suggests an 11.7-fold decrease in toxicity with respect to that of free DOX (0.41μM). In contrast, for HeLa cells that express a high level of heparanase, the IC_{50} of the Hep(DOX)SN gel (3.16 μM) was only 3.8 times of that of DOX (0.84 μM), indicating that the cytotoxicity of the Hep(DOX)SN gel is much closer to that of free DOX. Because of the covalent anchoring of DOX to the gel network, drug release from the Hep(DOX)SN gel, as well as from the PEG-DOX gel, is difficult. Therefore, the Hep(DOX)SN gel is compatible with NIH-3T3 cells, similarly to the reference PEG-DOX gel (Fig. 3c). This cell-specific cytotoxicity clearly correlates with the amounts of drug released from gel network due to the heparanase-induced cleavage of heparin chains.

View Article Online
DOI: 10.1039/C4SC01603C

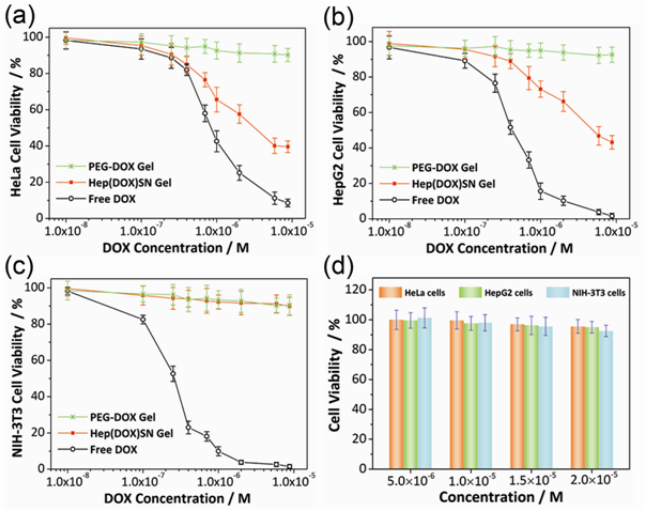

Fig. 3 Cell viability assay performed on (a) HeLa cells, (b) HepG2 cells, and (c) NIH-3T3 cells in the presence of the heparanase-responsive Hep(DOX)SN gel and the non-responsive PEG-DOX gel. (d) Cytotoxicity of HepSN against different cells. The cell viability was measured by MTT assays after 60 h incubation at 37°C.

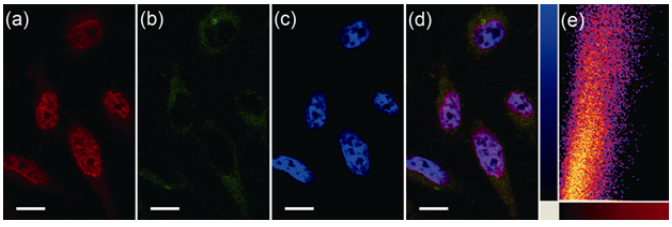

Fig. 4 Confocal images (maximum intensity projection) of HeLa cells incubated with Hep(DOX)SN gel for 20 h. (a) released drug, (b) lysosomes, (c) nucleus, (d) overlay, and (e) colocalization analysis between DOX and the nucleus calculated from individual fluorescence points. DOX (red), LysoTracker green DND-26 (green), DAPI (blue). The scale bars are 10 μm.

These findings are further supported by monitoring the intracellular distribution of the released drug using confocal

microscopy. As shown in Fig. 4a–d, after incubating HeLa cells with the Hep(DOX)SN gel for 20 h, a diffuse signal of released drug is observed in the nucleus of the cells. Colocalization analysis between DOX and the nucleus (Fig. 4e) confirms that a significant portion of DOX has escaped from the cytoplasm and has translocated to the nucleus. Meanwhile, in the case of HepG2 cells, the released drug is still mainly trapped in the cytoplasm (Fig. S16, ESI†), suggesting that the Hep(DOX)SN gel was able to release the drug in a cell-specific manner by responding to the environmental levels of heparanase. Therefore, our enzyme-responsive hydrogel holds great promise for developing an ideal carrier for safe, targeted, and sustained drug delivery.

Conclusions

In summary, we reported a novel enzyme-mediated redox initiation ternary system involving GOx, *N*-hydroxyimide compound and β-D-glucose. This initiation system enables the rapid formation of carbon-centered radicals that are capable of efficiently initiating chain polymerization at room temperature. By utilizing an *N*-hydroxyimide-heparin conjugate rationally designed to act as both an enzyme-mediated radical initiator and an enzyme-sensitive therapeutic carrier, we have prepared an enzyme-responsive hydrogel with tunable network properties via GOx-mediated radical polymerization. We demonstrated that the hydrogel containing drug molecules that are covalently anchored to the *N*-hydroxyimide-heparin conjugate can release the drug in an enzyme-responsive manner due to the heparin-specific cleavage by heparanase. The drug-loaded gel can target the cancer cells that are characterized by heparanase overexpression, and the use of this gel minimizes the adverse effects of premature drug release on normal cells. These enzyme-responsive hydrogels are potential for providing smart, multifunctional platforms that can adapt to a variety of microstructuring requirements for cell culturing, targeted cargo delivery, and regenerative medicine.

Acknowledgements

This research was supported by the National Natural Science Foundation of China (No. 21274111), the Program for New Century Excellent Talents in University of Ministry of Education of China (NECT-11-0386), the Fundamental Research Funds for Central Universities, and the Recruitment Program of Global Experts.

Notes and references

[a] Department of Chemistry, Advanced Research Institute, Tongji University, Shanghai 200092, China.
Email: wangqg66@tongji.edu.cn
[b] School of Stomatology, Tongji University, Shanghai 200092, China.

† Electronic Supplementary Information (ESI) available: Experimental details and supplementary figures. See DOI: 10.1039/b000000x/

1 A. M. Kloxin, A. M. Kasko, C. N. Salinas and K. S. Anseth, *Science*, 2009, **324**, 59-63.
2 C. Wang, Q. Chen, Z. Wang and X. Zhang, *Angew. Chem. Int. Ed.*, 2010, **49**, 8612-8615.
3 S. Himmelein, V. Lewe, M. C. A. Stuart and B. J. Ravoo, *Chem. Sci.*, 2014, **5**, 1054-1058.
4 K. Liang, J. J. Richardson, H. Ejima, G. K. Such, J. Cui and F. Caruso, *Adv. Mater.*, 2014, **26**, 2398-2402.
5 Y. Lan, Y. Wu, A. Karas and O. A. Scherman, *Angew. Chem. Int. Ed.*, 2014, **53**, 2166-2169.
6 D. S. Guo, K. Wang, Y. X. Wang and Y. Liu, *J. Am. Chem. Soc.*, 2012, **134**, 10244-10250.
7 M. P. Chien, M. P. Thompson, E. C. Lin and N. C. Gianneschi, *Chem. Sci.*, 2012, **3**, 2690-2694.
8 M. A. Azagarsamy and K. S. Anseth, *Angew. Chem. Int. Ed.*, 2013, **52**, 13803-13807.
9 K. A. Mosiewicz, L. Kolb, A. J. van der Vlies, M. M. Martino, P. S. Lienemann, J. A. Hubbell, M. Ehrbar and M. P. Lutolf, *Nat. Mater.*, 2013, **12**, 1072-1078.
10 C. A. DeForest and K. S. Anseth, *Nat. Chem.*, 2011, **3**, 925-931.
11 W. Cao, X. Zhang, X. Miao, Z. Yang and H. Xu, *Angew. Chem. Int. Ed.*, 2013, **52**, 6233-6237.
12 D. E. Whitaker, C. S. Mahon and D. A. Fulton, *Angew. Chem. Int. Ed.*, 2013, **52**, 956-959.
13 E. Cheng, Y. Xing, P. Chen, Y. Yang, Y. Sun, D. Zhou, L. Xu, Q. Fan and D. Liu, *Angew. Chem. Int. Ed.*, 2009, **48**, 7660-7663.
14 M. Nakahata, Y. Takashima, H. Yamaguchi and A. Harada, *Nat. Commun.*, 2011, **2**, 511.
15 Y. Kuang and B. Xu, *Angew. Chem. Int. Ed.*, 2013, **52**, 6944-6948.
16 A. M. Tang, W. J. Wang, B. Mei, W. L. Hu, M. Wu and G. L. Liang, *Sci. Rep.*, 2013, **3**, 1848.
17 E. A. Appel, X. J. Loh, S. T. Jones, F. Biedermann, C. A. Dreiss and O. A. Scherman, *J. Am. Chem. Soc.*, 2012, **134**, 11767-11773.
18 L. E. Buerkle, H. A. von Recum and S. J. Rowan, *Chem. Sci.*, 2012, **3**, 564-572.
19 J. Li, Y. Gao, Y. Kuang, J. Shi, X. Du, J. Zhou, H. Wang, Z. Yang and B. Xu, *J. Am. Chem. Soc.*, 2013, **135**, 9907-9914.
20 J. Raeburn, A. Zamith Cardoso and D. J. Adams, *Chem. Soc. Rev.*, 2013, **42**, 5143-5156.
21 S. K. M. Nalluri and R. V. Ulijn, *Chem. Sci.*, 2013, **4**, 3699-3705.
22 P. K. Vemula, G. A. Cruikshank, J. M. Karp and G. John, *Biomaterials*, 2009, **30**, 383-393.
23 Q. Wang, Z. Yang, X. Zhang, X. Xiao, C. K. Chang and B. Xu, *Angew. Chem. Int. Ed.*, 2007, **46**, 4285-4289.
24 W. S. Toh, T. C. Lim, M. Kurisawa and M. Spector, *Biomaterials*, 2012, **33**, 3835-3845.
25 L. S. Moreira Teixeira, J. Feijen, C. A. van Blitterswijk, P. J. Dijkstra and M. Karperien, *Biomaterials*, 2012, **33**, 1281-1290.
26 T. C. Lim, W. S. Toh, L.-S. Wang, M. Kurisawa and M. Spector, *Biomaterials*, 2012, **33**, 3446-3455.
27 L.-S. Wang, J. Boulaire, P. P. Y. Chan, J. E. Chung and M. Kurisawa, *Biomaterials*, 2010, **31**, 8608-8616.
28 R. Shenoy and C. N. Bowman, *Biomaterials*, 2012, **33**, 6909-6914.
29 P. S. Hume, C. N. Bowman and K. S. Anseth, *Biomaterials*, 2011, **32**, 6204-6212.
30 T. Su, D. Zhang, Z. Tang, Q. Wu and Q. Wang, *Chem. Commun.*, 2013, **49**, 8033-8035.
31 R. Shenoy, M. W. Tibbitt, K. S. Anseth and C. N. Bowman, *Chem. Mater.*, 2013, **25**, 761-767.
32 L. M. Johnson, C. A. DeForest, A. Pendurti, K. S. Anseth and C. N. Bowman, *ACS Appl. Mater. Interf.*, 2010, **2**, 1963-1972.

View Article Online
DOI: 10.1039/C4SC01603C

33 L. M. Johnson, B. D. Fairbanks, K. S. Anseth and C. N. Bowman, *Biomacromolecules*, 2009, **10**, 3114-3121.
34 I. Capila and R. J. Linhardt, *Angew. Chem. Int. Ed.*, 2002, **41**, 390-412.
35 J. M. Whitelock and R. V. Iozzo, *Chem. Rev.*, 2005, **105**, 2745-2764.
36 K. E. Hunter, C. Palermo, J. C. Kester, K. Simpson, J. P. Li, L. H. Tang, D. S. Klimstra, I. Vlodavsky and J. A. Joyce, *Oncogene*, 2014, **33**, 1799-1808.
37 S. Simizu, K. Ishida, M. K. Wierzba, T. A. Sato and H. Osada, *Cancer Lett.*, 2003, **193**, 83-89.
38 I. Lerner, L. Baraz, E. Pikarsky, A. Meirovitz, E. Edovitsky, T. Peretz, I. Vlodavsky and M. Elkin, *Clin. Cancer Res.*, 2008, **14**, 668-676.
39 S. R. S. Ting, J. M. Whitelock, R. Tomic, C. Gunawan, W. Y. Teoh, R. Amal and M. S. Lord, *Biomaterials*, 2013, **34**, 4377-4386.
40 M. F. Maitz, U. Freudenberg, M. V. Tsurkan, M. Fischer, T. Beyrich and C. Werner, *Nat. Commun.*, 2013, **4**, 2168.
41 I.-K. Park, Y. J. Kim, T. H. Tran, K. M. Huh and Y. Lee, *Polymer*, 2010, **51**, 3387-3393.
42 M. V. Tsurkan, K. Chwalek, S. Prokoph, A. Zieris, K. R. Levental, U. Freudenberg and C. Werner, *Adv. Mater.*, 2013, **25**, 2606-2610.
43 P. M. Kharkar, K. L. Kiick and A. M. Kloxin, *Chem. Soc. Rev.*, 2013, **42**, 7335-7372.
44 Z. Zhang, S. A. McCallum, J. Xie, L. Nieto, F. Corzana, J. Jiménez-Barbero, M. Chen, J. Liu and R. J. Linhardt, *J. Am. Chem. Soc.*, 2008, **130**, 12998-13007.
45 B. D. Fairbanks, M. P. Schwartz, A. E. Halevi, C. R. Nuttelman, C. N. Bowman and K. S. Anseth, *Adv. Mater.*, 2009, **21**, 5005-5010.
46 B. A. Holmén, M. I. Tejedor-Tejedor and W. H. Casey, *Langmuir*, 1997, **13**, 2197-2206.
47 K. M. Park, J. A. Yang, H. Jung, J. Yeom, J. S. Park, K. H. Park, A. S. Hoffman, S. K. Hahn and K. Kim, *ACS Nano*, 2012, **6**, 2960-2968.
48 B. J. Berron, L. M. Johnson, X. Ba, J. D. McCall, N. J. Alvey, K. S. Anseth and C. N. Bowman, *Biotechnol. Bioeng.*, 2011, **108**, 1521-1528.
49 S. Trivić, V. Leskovac, J. Zeremski, M. Vrvić and G. W. Winston, *Bioorg. Chem.*, 2002, **30**, 95-106.
50 V. Leskovac, S. Trivić, G. Wohlfahrt, J. Kandrač and D. Peričin, *Int. J. Biochem. Cell Biol.*, 2005, **37**, 731-750.
51 L.-S. Wang, C. Du, W. S. Toh, A. C. Wan, S. J. Gao and M. Kurisawa, *Biomaterials*, 2014, **35**, 2207-2217.
52 J. Thiele, Y. Ma, S. M. C. Bruekers, S. Ma and W. T. S. Huck, *Adv. Mater.*, 2014, **26**, 125-148.